XL CILAMCE
IBERO-LATIN AMERICAN
CONGRESS ON
COMPUTATIONAL
METHODS IN
ENGINEERING

NOVEMBER
11-14, 2019
Praiamar Natal Hotel & Convention
Natal, RN-BRAZIL

NUMERICAL AND EXPERIMENTAL ANALYSIS OF THE CHEVRON NOTCHED BRAZILIAN DISC

João Marcelo M. Guimarães
Lourdes M. S. Souza
Marlon A. A. C. Nunes
Deane Roehl
joaomarcelo@tecgraf.puc-rio.br
lmsilvadesouza@tecgraf.puc-rio.br
marlonaugustus@tecgraf.puc-rio.br
deane@tecgraf.puc-rio.br
Tecgraf Institute / PUC-Rio, Civil Engineering Department / PUC-Rio
Marquês de São Vicente Street, 225, 22453-900, Rio de Janeiro, Rio de Janeiro, Brazil.

Abstract. The Linear Elastic Fracture Mechanics (LEFM) tries to describe the fracture and damage phenomena in materials that obey Hooke´s law. However some small scale plasticity can be bypassed. The main studies in the fracture mechanics area come from the energy balance of Griffith, in 1920 and some improvement with the energy release rate added by Irwin, in 1956. Rocks often features structural defects, including flaws, cracks, cleavages and natural fractures. Fracture toughness represents the capability of fragile materials, such as rocks and concretes, containing initial cracks to resist further fracturing. A widely used test that provide this information to model fracture propagation is the Cracked Chevron Notched Brazilian Disc (CCNBD). Nevertheless, there is some discussion about the precision of this test. In this study, mortar specimens had their fracture toughness experimentally assessed by the CCBND method. Numerical fracture analyses were carried out using the Extended Finite Element Method (XFEM) trying to reproduce the CCNBD test comparing with the experimental results aiming to better understand this test. Results indicate that the CCNBD test underestimates the fracture toughness in about 13%.

Keywords: CCNBD, Fracture toughness, XFEM.

1 Introduction

Concrete and rock are widely used materials in Engineering. One of the main concerns related to these materials is their quasi-brittle behavior under low confining stresses. As an attempt to describe the mechanical behavior of quasi-brittle materials, fracture mechanics comes to model the formation and propagation of fractures. The main studies in this area come from the energy balance of Griffith, in 1920 [1]. Some improvement with the energy release rate was added by Irwin, in 1956 [2]. In this scope, fracture toughness for mode I (opening in tension) is a common failure mode.

The Cracked Chevron Notched Brazilian Disc (CCNBD) is a method suggested by ISRM for determining mode I fracture toughness of brittle materials. Discrepancy has been observed in comparison to other methods. Some authors pointed out that this can be partially ascribed to the fact that the fracture profile disagrees with the assumed straight through crack front [3] Figure 1 shows a schematic of the CCNBD specimen under compression. According to the theory behind the Brazilian test, radial compression of a disc will induce tension stresses in the geometrical center of the specimen. Therefore a Chevron notch is made in the center, in order to induce the formation and propagation of a stable mode I fracture. When the peak load is reached the fracture features a stable-unstable transition accompanied by the transition of increasing followed by decreasing loading force [4].

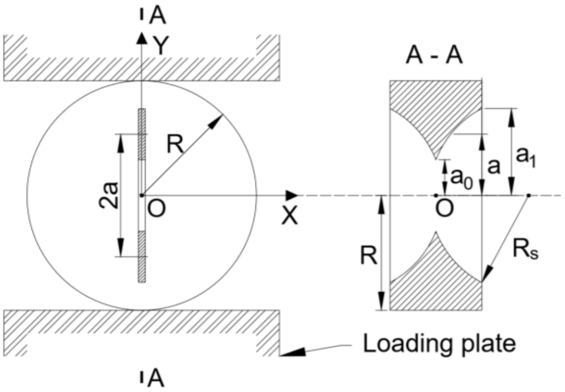

R = radius of Brazilian disc specimen
a_0=initial chevron notched crack length
a_1=final chevron notched crack length
a=crack length
R_s=saw radius

Figure 1. CCNBD specimen geometry(based on [5]).

The mode I fracture toughness K_{IC} can be determined by:

$$K_{Ic} = \frac{P_{max}}{B \cdot \sqrt{D}} \cdot Y^*_{min} \qquad (1)$$

Where B is the specimen thickness, D is the specimen diameter. Y^*_{min} is a geometrical parameter that depends on α_0 (=a_0/R), α_1 (=a_1 /R) and α_B (=B/R) and gives the minimum stress intensity factor. It reaches its minimum value once the effect of the increasing crack length overshadows that of the increasing crack front width, and the crack develops unstably [6]. The Y^*_{min}value can be calculated using ISRM suggested method [5] or the recalibration made by Wang [6]. In this work we used Wang´s calculation [6] to determine the Y^*_{min} value. In this paper, experimental and numerical analyses have been conducted on the CCNBD tests aiming at better understanding the processes featured in this test.

2 Experimental Procedure

Mortar specimens were casted in cylinders with 75mm of diameter and 65mm of height with a thin piece of Polystyrene foam in the shape of the notch centered in the molds. This method provided notches with thickness between 1.0mm to 1.5mm. The mortars were prepared with cement CPV from Holcim, river sand with D_{max} of 1.18 mm and tap water. The specimens were demolded after 1 day of curing at room temperature and tested after 2 days. The CCNBD tests were carried out in a servo-hydraulic testing machine from MTS model 810 with 500 kN of load capacity, under piston displacement control at a rate of 0.05mm/min. In order to obtain the Young's modulus and Poisson's ratio, uniaxial compressive tests were performed in the same testing machine, under piston displacement control at a rate of 0.08mm/min. Axial and circumferential strains were measured by LVDTs. Brazilian splitting tests were performed to measure the splitting tensile strength in the same test machine. A clip gauge was attached to the center of the specimen and the tests were performed under crack opening displacement control at a rate of 0.01mm/min. In addition, cyclic three-point bending tests were performed on three specimens with 40 x 40 x 160 mm (span length = 150 mm) in the same test machine. The tests had 5 cycles and fracture toughness calculations followed recommendations by RILEM[7].

3 Numerical modeling

The computational analyses were carried out using the commercial software Abaqus®. The analyses were conducted with the Extended Finite Element Method (XFEM) [8][9]. XFEM fractures can propagate across elements without the need to update the mesh during the process. Crack initiation was modeled with the criteria of maximum principal stress. An additional crack is introduced each time the stress reaches the maximum stress allowed within a given tolerance. Damage evolution was modeled based on the energy released during the damage process, this means (G=$G_{critical}$). In this work, the model was discretized with 3D, 8-node, linear brick elements. The Young's modulus, Poisson's ratio and splitting tensile strength were obtained from the experiments: 25 GPa, 0.21 and 4.0MPa, respectively. All models considered specimens with diameter (D) of 75 mm, thickness (B) of 30 mm and notch width of 1.5mm while α_0, α_1 and α_B are 0.2613, 0.6317 and 0.8, respectively.

4 Experimental Results

The typical force versus displacement curve obtained from experiments is shown in Fig. 3 and the mean peak load and fracture toughness are in Table 2. The load slowly increases until the peak, when it drops quickly. Some samples regained load capacity after the critical value because when the disc is split, the two semicircular pieces can still bear compression like two pillars.

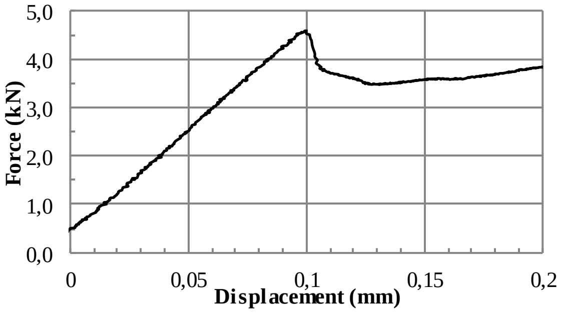

Figure 3. Typical curve of the CCNBD tests.

Table 2. Average peak load, specimen thickness and diameter, Y^*_{min} and fracture toughness from the CCBND tests. The fracture toughness values calculated from Wang's formula [6].

P_{max}(kN)	B (mm)	D (mm)	Y^*_{min}	K_{IC} (MPa $\cdot\sqrt{\text{m}}$)
4.40 ± 0.16	30.0	72.52 ± 0.55	0.9417 ± 0.0237	0.5128 ± 0.0136

5 Numerical analyses

One of the parameters of the model, the fracture energy was obtained from the K_{IC} values and the relation $G_f = {K_{IC}}^2/E$. The calculated fracture energy and other model parameters are presented in Table

3. In the numerical models, the effects of fracture energy, mesh size, load distribution, fracture initiation and integration type were evaluated and the resulting curves are shown in Fig. 4.

All models featured a sharp decrease in the load after P_{max}, when the fracture reached the end of the notch. This happens because there is a stable-unstable transition in the fracture propagation, according to literature.[3][6] It was also noted a relative low change in the peak force and inclination which can be seen as a consistency in the solution.

Table 3. Parameters varied in the models and the resulting peak forces.

Model	Fracture energy (MPa*mm)	Approximate mesh global size (mm)	Force distribution	XFEM fracture initiation	Integration type	Resulting Peak force (kN)
A	0.01051	3	linear	yes	reduced	3.707
B	0.01051	1	linear	yes	reduced	3.693
C	0.01051	3	6°	yes	reduced	3.852
D	0.01051	3	6°	No	reduced	3.852
E	0.01051	3	6°	yes	Full	3.927
F	0.01395	3	6°	yes	reduced	4.284

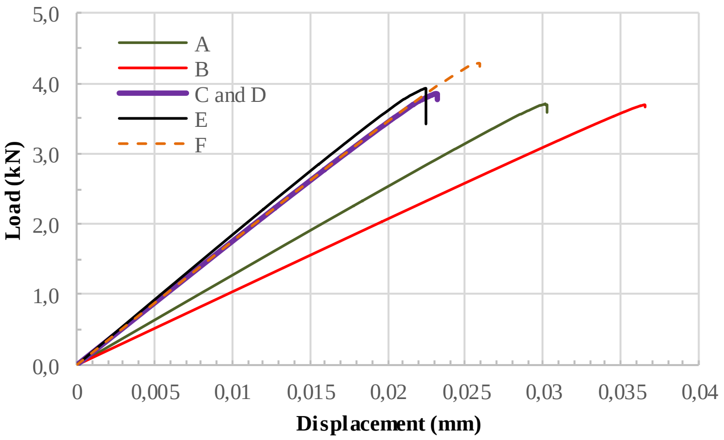

Figure 4. Load versus displacement for all considered numerical models

The influence of the load distribution was evaluated, comparing models A and C. In model A, the load was applied on a line on the top of the disc (Fig. 5(a)) whereas in model C, the load was applied on an area with a 6° angle of the circumference, as shown in Fig. 5(b). It was observed that model C resulted in a greater inclination and peak force than model A. Once the load is better distributed, smaller strains and a higher peak force are expected. The effect of mesh-size was evaluated with models A and B. In model A, the approximate global element size was about 3mm whereas in Model B, a smaller element-size (1mm) was used. The variation in peak load was very small while the specimen stiffness was very sensitive to element size. The influence of imposed fracture initiation was also studied. In model D, fracture initiation was imposed while in model C, it was not. The obtained results were the same. As predicted by the theory of the test, the fracture initiates at the notch tip. The integration type was also evaluated by comparing models C and E – the former with reduced integration while the latter with full integration. The full integration gave a stiffer response with a higher peak load, as expected. Lastly, in model F, we used the mean fracture energy obtained from the three-point bending test (0.01395 ± 0.00103 MPa*mm). The peak load obtained with this model was very close to the experimental peak load during the CCNBD test. This could indicate that CCNBD test may underestimate K_{IC}, due to the fact that the crack is assumed straight in the model, differently from what was experimentally observed.

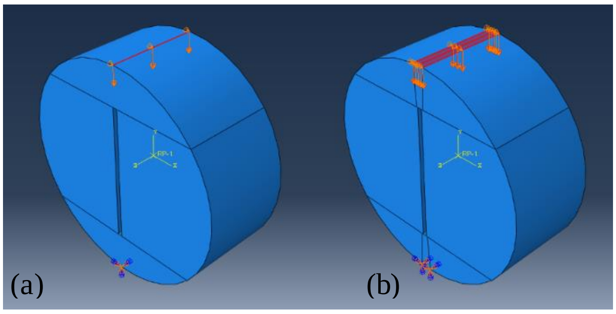

Figure 5. Boundary conditions: (a) – force applied on a line on the top of the specimen (b) – force applied on a 6 degree area on the top of the specimen.

6 Conclusion

This experimental-numerical work had the goal to contribute towards better understanding the CCNBD test by comparing experimental and numerical results. A parametric study was conducted where the influence of mesh size, force distribution, fracture initiation and integration type was evaluated. Mesh size and integration type had limited influence on the results. A numerical analysis using XFEM and a small contact area was able to initiate fracture at the crack tip and propagate fracture through a plausible path even without predetermined fracture initiation. It presented a peak load 12% lower than the experimental average value. However, when the value of fracture energy provided by the three-point bending test was considered, the model provided a peak load close to experimental data. This may indicate that the CCNBD experimental test underestimates the fracture energy in about 25% and fracture toughness in about 13%.

References

[1] Griffith, A. A. The phenomena of rupture and flow in solids. Trans. R. Soc. London A, 1920.
[2] Irwin, G. R. Analysis of stresses and strains near the end of a crack traversing a plate. 1957.
[3] Y. Xu, F. Dai, T. Zhao, N. wen Xu, and Y. Liu. Fracture Toughness Determination of Cracked Chevron Notched Brazilian Disc Rock Specimen via Griffith Energy Criterion Incorporating Realistic Fracture Profiles. *Rock Mech. Rock Eng*, vol. 49, no. 8, pp. 3083–3093, 2016.
[4] F. Dai, M. D. Wei, N. W. Xu, Y. Ma, and D. S. Yang. Numerical Assessment of the Progressive Rock Fracture Mechanism of Cracked Chevron Notched Brazilian Disc Specimens *Rock Mech. Rock Eng*, vol. 48, no. 2, pp. 463–479, 2014.
[5] R. J. Fowell. Suggested Method for Determining Mode I Fracture Toughness Using Cracked Chevron Notched Brazilian Disc (CCNBD) Specimens," *ISRM*, vol. 32, no. I, pp. 57–64, 1995.
[6] Q. Z. Wang, H. Fan, X. P. Gou, and S. Zhang. Recalibration and Clarification of the Formula Applied to the ISRM-suggested CCNBD Specimens for Testing Rock Fracture Toughness. *Rock Mech. Rock Eng.*, vol. 46, no. 2, pp. 303–313, 2013.
[7] S. P. Shah. Determination of Fracture Parameters (K Ic s and CTOD c) of Plain Concrete Using Three-Point Bend Tests.," *Mater. Struct.*, vol. 23, pp. 457–460, 1991.
[8] N. Sukumar and J. H. Prévost. Modeling Quasi-Static Crack Growth with the Extended Finite Element Method Part I: Computer implementation," *Int. J. Solids Struct.*, vol. 40, no. 26, pp. 7513–7537, 2003.
[9] Belytschko T, Black T. Elastic crack growth in finite elements with minimal remeshing. International Journal for Numerical Methods in Engineering, 45:601-20, 1999.